

# Using solid-state $^{31}\text{P}\{^{19}\text{F}\}$ REDOR NMR to measure distances between a trifluoromethyl group and a phosphodiester in nucleic acids

Elizabeth A. Louie, Panadda Chirakul, Vinodhkumar Raghunathan, Snorri Th. Sigurdsson<sup>1</sup>, Gary P. Drobny\*

University of Washington, Chemistry Department, Campus Box 351700, Seattle, WA 98195-1700, USA

Received 6 March 2005; revised 25 June 2005

Available online 4 October 2005

## Abstract

REDOR is a solid-state NMR technique frequently applied to biological structure problems. Through incorporation of phosphorothioate groups in the nucleic acid backbone and mono-fluorinated nucleotides,  $^{31}\text{P}\{^{19}\text{F}\}$  REDOR has been used to study the binding of DNA to drugs and RNA to proteins through the detection of internuclear distances as large as 13–14 Å. In this work,  $^{31}\text{P}\{^{19}\text{F}\}$  REDOR is further refined for use in nucleic acids by the combined use of selective placement of phosphorothioate groups and the introduction of nucleotides containing trifluoromethyl ( $-\text{CF}_3$ ) groups. To ascertain the REDOR-detectable distance limit between a unique phosphorous spin and a trifluoromethyl group and to assess interference from intermolecular couplings, a series of model compounds and DNA dodecamers were synthesized each containing a unique phosphorous label and trifluoromethyl group or a single  $^{19}\text{F}$  nucleus. The dipolar coupling constants of the various  $^{31}\text{P}$  and  $^{19}\text{F}$  or  $-\text{CF}_3$  containing compounds were compared using experimental and theoretical dephasing curves involving several models for intermolecular interactions.

© 2005 Published by Elsevier Inc.

**Keywords:** Solid-state nuclear magnetic resonance;  $^{31}\text{P}\{^{19}\text{F}\}$  REDOR; Rotational-echo double resonance; Dipolar recoupling; Internuclear distance; Trifluoromethyl group

## 1. Introduction

Solid-state nuclear magnetic resonance (NMR) spectroscopy is widely used to study the structure of biomolecules and biological complexes that are not easily crystallized or dissolved, and thus cannot be conveniently studied by X-ray crystallography and solution-state NMR, respectively. The distance range accessible by REDOR generally exceeds that of NOE or residual dipolar coupling measurements, therefore structural features that must be derived indirectly from short range distance measurements using NOE data can often be

directly observed using REDOR [1,2]. For example,  $^{31}\text{P}\{^{19}\text{F}\}$  REDOR has been implemented to measure direct changes in long-range protein structure upon ligand binding [3], and changes in minor groove width of DNA oligomers upon binding distamycin [4,5] with reported  $^{31}\text{P}$  to  $^{19}\text{F}$  internuclear distances of approximately 16 and 13.5 Å, respectively. These are among the longest internuclear distances measured by NMR methods.

The heteronuclear dipolar coupling constant  $D_{IS}$  is directly related to the gyromagnetic ratio ( $\gamma_I, \gamma_S$ ) of the two spins ( $I, S$ ) of interest and inversely proportional to the cube of the internuclear distance  $r_{I-S}$ :  $D \propto \gamma_I \gamma_S / r_{I-S}^3$ . Therefore, nuclear spins with larger magnetic moments, and thus the larger gyromagnetic ratios, will result in larger dipolar coupling constants for a given distance than nuclear spins with smaller gyromagnetic ratios. The  $^{13}\text{C}$  nucleus is a mainstay for solid-state

\* Corresponding author. Fax: +1 206 685 8665.

E-mail addresses: [snorrisi@hi.is](mailto:snorrisi@hi.is) (S.Th. Sigurdsson), [drobny@chem.washington.edu](mailto:drobny@chem.washington.edu) (G.P. Drobny).

<sup>1</sup> Present address: University of Iceland, Science Institute, Dunhaga3, IS-107 Reykjavik, Iceland.

distance measurements, with the longest  $^{13}\text{C}$  distances measured by dipolar recoupling in the neighborhood of 6 Å [3], corresponding to a dipolar coupling of about 35 Hz. In contrast,  $^{19}\text{F}$  has a gyromagnetic ratio over 3.5 times the size of  $^{13}\text{C}$  and two  $^{19}\text{F}$  spins separated by 6 Å have a dipolar coupling of over 490 Hz, while two  $^{19}\text{F}$  spins separated by 14.5 Å have a dipolar coupling of about 35 Hz. But in practice,  $^{19}\text{F}$ – $^{19}\text{F}$  homonuclear recoupling seems limited, at least in nucleic acids, to a maximum distance range of 9–10 Å [6]; recent work by McDermott and co-workers [7] using linear polymers with distally attached trifluoromethyl groups advanced that limit to about 12 Å. A complication that may arise in  $^{19}\text{F}$ – $^{19}\text{F}$  recoupling that is at least partly responsible for the attenuated upper limit of distance measurement is incomplete decoupling of  $^{19}\text{F}$ – $^1\text{H}$  dipolar interactions.

For the purpose of measuring internuclear distances greater than 12 Å,  $^{31}\text{P}\{^{19}\text{F}\}$  REDOR has shown considerable promise. A  $^{31}\text{P}$  spin, with a somewhat smaller magnetic moment, separated by 11 Å from a  $^{19}\text{F}$  spin has a dipolar coupling of about 35 Hz. Due to the smaller magnetic moment and because most biologically relevant  $^{31}\text{P}$  spins are in phosphate groups,  $^{31}\text{P}$ – $^1\text{H}$  decoupling during  $^{31}\text{P}\{^{19}\text{F}\}$  REDOR is not as problematic as  $^{19}\text{F}$ – $^1\text{H}$  decoupling during  $^{19}\text{F}$ – $^{19}\text{F}$  recoupling. The long  $T_2$  of  $^{31}\text{P}$  under conditions of the REDOR experiment enables the measurement of  $^{31}\text{P}$ – $^{19}\text{F}$  distances of up to 16 Å ( $D_{IS} = 11$  Hz) as demonstrated by Schaefer and co-workers [3] in a study of a complex of the enzyme 5-enolpyruvylshikimate-3-phosphate (EPSP) and shikimate-3-phosphate (S3P).

In nucleic acids, and especially in DNA, the redundancy of the phosphodiester in the backbone results in a poorly resolved  $^{31}\text{P}$  NMR spectrum [4]. To enable site-specific detection of  $^{31}\text{P}$ – $^{19}\text{F}$  distances during REDOR, a single phosphate group in DNA or RNA is replaced by a phosphorothioate group. The  $^{31}\text{P}$  in a phosphorothioate group is shifted approximately 55 ppm from the  $^{31}\text{P}$  phosphate group signal in DNA and RNA [4]. Selective placement of phosphorothioate groups in combination with  $^{19}\text{F}$ -substituted nucleotides allows detection of  $^{31}\text{P}$ – $^{19}\text{F}$  distances site specifically.  $^{31}\text{P}$ – $^{19}\text{F}$  distances spanning the minor groove of a DNA oligomer have been measured as a function of distamycin–DNA binding stoichiometry [5], and for 2:1 drug:DNA binding stoichiometry a 13.5 Å ( $D_{IS} = 19$  Hz) distance was determined [5].

Even the 16 Å limit achieved by  $^{31}\text{P}\{^{19}\text{F}\}$  may be insufficient for some applications, and the acquisition time necessary to observe the effect of weak  $^{31}\text{P}$ – $^{19}\text{F}$  dipolar couplings in a REDOR experiment may prove impractical in some cases. For example, it may prove desirable to measure changes in the major groove width of DNA, or changes in RNA tertiary structure as a result of protein binding. Such experiments may require measurement of  $^{31}\text{P}$ – $^{19}\text{F}$  distances of 16 Å or more. Also, although mea-

surement of  $^{31}\text{P}$ – $^{19}\text{F}$  dipolar couplings in the 12–16 Å range is feasible, in some cases REDOR measurements are susceptible to interference from intermolecular couplings. One way to extend the range of  $^{31}\text{P}$  REDOR is to dephase  $^{31}\text{P}$  spins with the fluorines of a trifluoromethyl ( $\text{CF}_3$ ) group. For instance, if an isolated  $^{31}\text{P}$ – $^{19}\text{F}$  spin pair is separated by 16 Å, the corresponding dipolar coupling constant is about 11 Hz. The corresponding amount of REDOR dephasing is 11% at 30 ms. If instead the  $^{31}\text{P}$  spin is coupled to the three  $^{19}\text{F}$  spins of a rapidly rotating trifluoromethyl group, REDOR data roughly equivalent to the 16 Å  $^{31}\text{P}$ – $^{19}\text{F}$  pair are achieved for a distance of 19 Å between the  $^{31}\text{P}$  spin and the “pseudo-atom” center of the trifluoromethyl group. Recently, Schaefer and co-workers [8] have determined the conformation of a bound trifluoromethylketal substituted shikimate-based bisubstrate inhibitor ( $\text{CF}_3$ -SBBi) to EPSP using  $^{31}\text{P}\{^{19}\text{F}_3\}$  REDOR and measured a distance of 8.3 Å. ( $\{^{19}\text{F}_3\}$  is used to designate the dephasing of the three fluorines from a rotating  $-\text{CF}_3$  group.) However, a distance of less than 12 Å is believed to be somewhat moderate for recoupling  $^{31}\text{P}$  to the  $^{19}\text{F}$  spin of a rotating  $-\text{CF}_3$  group due to its high gyromagnetic ratio. Thus, investigating the limitations of dipolar recoupling of  $^{31}\text{P}$  and  $^{19}\text{F}$  of a rotating  $-\text{CF}_3$  group is worth exploring when structural information is desired at the molecular level for large biomolecular systems.

The basic principles of REDOR dephasing by multiple spins in the presence of molecular motion have been discussed by Goetz and Schaefer [9], with specific reference to  $^{13}\text{C}$  spins dephased by  $-\text{CF}_3$  groups. A primary feature of this type of REDOR is that even though the  $^{19}\text{F}$  spins are strongly dipolar coupled, the equality of the averaged  $^{31}\text{P}$ – $^{19}\text{F}$  dipolar couplings which results from the rotation of the trifluoromethyl group removes the effect of the  $^{19}\text{F}$ – $^{19}\text{F}$  couplings from the REDOR data, at least to second order. Therefore,  $^{31}\text{P}\{^{19}\text{F}_3\}$  REDOR has excellent prospects for applications in nucleic acid problems where a long-range distance measurement is desired.

In this work, we accomplish two objectives. First, we demonstrate the degree of perturbation introduced by trifluoromethyl groups by comparative measurements of DNA helix stability and by direct comparison of distances measured in DNA by  $^{31}\text{P}\{^{19}\text{F}_3\}$  REDOR. Second, we use model compound studies and simulations to assess the degree of interference in REDOR measurements from intermolecular  $^{31}\text{P}$ – $^{19}\text{F}_3$  dipolar couplings.

## 2. Materials and methods

### 2.1. General

The first four model compounds (1–4) shown in Fig. 1 were synthesized from 4-fluorophenol (1a),

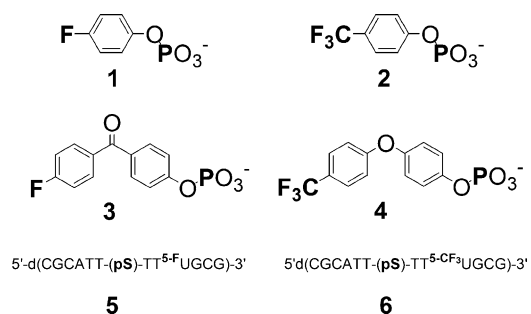


Fig. 1. Compounds and molecules (1–6) with unique phosphorous and –F or –CF<sub>3</sub> group, used in this study where the distance between the phosphorous atom and –F or –CF<sub>3</sub> were measured by <sup>31</sup>P{<sup>19</sup>F} REDOR.

$\alpha,\alpha,\alpha$ -trifluoro-*p*-cresol (**2a**), 4-fluoro-4-hydroxybenzophenone (**3a**), and 4-4-(trifluoromethyl)phenoxyphenol (**4a**), which were purchased from Aldrich. Ethylthiotetrazole and 2-cyanoethyl diisopropylchlorophosphoramidite were purchased from Glen Research and Chem Genes, respectively. Acetonitrile and dichloromethane were dried over calcium hydride followed by distillation under argon. Fig. 2 shows the general scheme for the synthesis of compounds 1–4. In general, all reactions were run under argon atmosphere unless otherwise noted. Flash column chromatography was carried out with EM type 60 (230–400 mesh) silica gel. Cation exchange chromatography was performed on MP-50 resin, grade 100–20 mesh, hydrogen form which was pre-treated with water, 1.00 N NaOH, then neutralized with water until pH 7.0. Preparative RP-HPLC separations were performed using a Dynamax C18 column (Rainin, 25 cm, 4.6 mm ID, 5  $\mu$ m, 300 Å) and the solvent gradients for preparative separation, RP-HPLC were run at 10 mL/min as follows: Gradient A: solvent A, 100 mM Et<sub>3</sub>NHOAc (pH 7.0); solvent B, CH<sub>3</sub>CN; 92% A for initial, 12 min linear gradient to 61% A, 8 min linear gradient to 30% A, isocratic for 3 min, 3 min linear gradient to initial conditions. Gradient B: the same as gradient

A except 95% A for initial, 15 min linear gradient to 30% A, isocratic for 10 min, then a 5 min linear gradient to initial conditions.

## 2.2. Synthesis and purification of fluorinated DNA oligomers (5 and 6) and their complementary sequence

The DNA, 5'-d(CGCATT-(pS)-TT-<sup>5-F</sup>U-GCG)-3' (**5**), 5'-d(CGCATT-(pS)-TT-<sup>5-CF<sub>3</sub></sup>U-GCG)-3' (**6**), and 5'-(dC GCAAAAATGCG)-3', were synthesized on an Applied Biosystems Model 394 synthesizer. DNA incorporated with 5-fluoro-2'-deoxyuridine was achieved by using 5'-(4,4'-dimethoxytrityl)-3'-(cyanoethyl)phosphoramidite-2'-deoxy-5-(fluoromethyl)uridine (Glen Research). The usual acetyl (Ac) protected dT, dG, dA, and dC CE phosphoramidites (Glen Research) were used. The DNA incorporated with the –CF<sub>3</sub> group was synthesized with 5'-(4,4'-dimethoxytrityl)-3'-(cyanoethyl)phosphoramidite-2'-deoxy-5-(trifluoromethyl)uridine [10–12], while using PAC-phosphoramidites and mild deprotection [12].

Incorporation of phosphorothioates into DNAs was done at the oxidation step in which a sulfurizing agent (Glen Research) is used in place of iodine solution. DNAs were deprotected and cleaved from the resin by using concentrated aqueous ammonia at 55 °C for 16 h. DNA were purified by HPLC (gradient and solvent: 10  $\mu$ mol DNA was brought up to 8 mL by 100 mM Et<sub>3</sub>NHOAc prep-HPLC: buffer A, 100 mM Et<sub>3</sub>NHOAc; buffer B, acetonitrile, 10 mL/min,  $\lambda$  260, 2 ml loop: 0–13 min at 2% B, 13–25 min at 2–15% B, 25–35 min at 15–35% B, 35–48 min at 35% B, 48–53 min at 35–2% B, and 53–62 min at 2% B).

## 2.3. Sample preparation for NMR studies

### 2.3.1. Model compounds

To dilute the spins, 5–10 mg of 1–4 was dissolved in deionized water and diluted with solutions of KBr and/or benzoic acid, lyophilized, and packed in a 5 mm rotor.

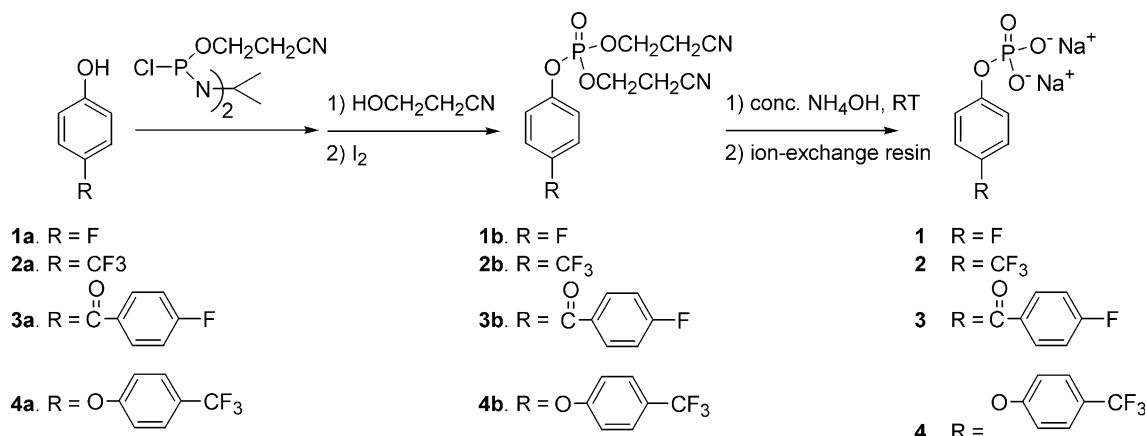


Fig. 2. Synthetic pathway of compounds 1–4.

Sixty microliters of H<sub>2</sub>O was added to 5 mg (**3**) and the liquid sample was then placed in a 5 mm rotor with tight end caps.

### 2.3.2. DNA samples

The DNAs were salted with 10% (w/w) NaCl and 10% (w/w) Na<sub>2</sub>EDTA, annealed at 85 °C for 10 min, lyophilized, and packed in 5 mm ceramic rotors, and placed in an 85% hydration chamber to yield at least 11 waters per nucleotide by weight which ensures that the DNA is in B-form [13].

### 2.3.3. NMR spectroscopy

All <sup>31</sup>P{<sup>19</sup>F} REDOR experiments were performed on a 4.7 T (200 MHz proton Larmor frequency) magnet, homebuilt MAS triple resonance (<sup>1</sup>H, <sup>19</sup>F, and <sup>31</sup>P) probe [6,14], and homebuilt console (J. Gladden and G.P. Drobny, Unpublished work). The <sup>1</sup>H π/2 pulse was set at 5 μs and the <sup>31</sup>P and <sup>19</sup>F π pulses were 10 and 7 μs, respectively. The <sup>1</sup>H and <sup>31</sup>P cross-polarization (CP) time was 2 ms. <sup>1</sup>H decoupling was set at 100–120 kHz during evolution and 80 kHz during acquisition [15–17]. Hydrated DNA or samples diluted in water were run at low temperature which ranged from –16 to –27 °C with a spinning speed of 5988 Hz. The model compounds **1–4** were spun at 4505, 5000 or 5988 Hz. The pulse sequence employed was XY8-REDOR [18] as shown in Fig. 3. Following generation of

<sup>31</sup>P magnetization by CP from the protons, the <sup>31</sup>P's are subjected to a series of 180° refocusing pulses. This full-echo spectrum is designated S<sub>0</sub>. In the second half of the experiment, in addition to the <sup>31</sup>P refocusing pulses, <sup>19</sup>F 180° pulses are added at the middle of the rotor period. These fluorine dephasing pulses reintroduce <sup>31</sup>P–<sup>19</sup>F dipolar couplings averaged by magic angle spinning (MAS), and cause a dephasing of the observed <sup>31</sup>P signal. The second half of the spectrum is referred to as S, and the ratio of S/S<sub>0</sub> provides a dephasing curve that can be fit to theoretical equations [1,2] which directly yields the dipolar coupling, D<sub>PF</sub>, between the <sup>31</sup>P and <sup>19</sup>F spins. Given the D<sub>PF</sub>, the internuclear distance, r<sub>PF</sub>, can be easily calculated from  $r_{PF} = [(\gamma_P \gamma_F h) / 4\pi^2 D_{PF}]^{1/3}$  where γ<sub>P</sub> and γ<sub>F</sub> are the gyromagnetic ratios of the P and F spins, respectively, h is Planck's constant, and D is the dipolar coupling in Hertz.

<sup>19</sup>F observe <sup>31</sup>P dephase REDOR cannot be exploited due to short T<sub>2</sub> relaxation of the <sup>19</sup>F nucleus [19]. Pan reports that after eight-rotor cycles of dephasing the fluorine signal is nearly completely dephased on a fluoroapatite crystal [19]. Dephasing on the <sup>31</sup>P nucleus would only be feasible for the small model compounds and not the dsDNA due to the dephasing contribution of <sup>31</sup>P nuclei in the phosphate backbone, and thus, the presence of multiple spin dephasers.

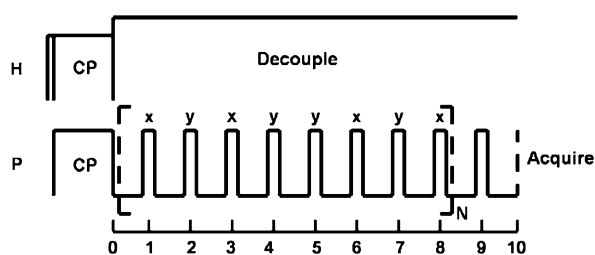
Goetz and Schaefer [9] presented closed form numerical algorithms for REDOR dephasing by multiple spins in the presence of molecular motion. The calculation assumes that the <sup>19</sup>F–<sup>19</sup>F homonuclear interaction does not affect REDOR dephasing. For a trifluoromethyl group, fast rotation about the threefold symmetry axis of the CF<sub>3</sub> group ensures that the three fluorine nuclei have identical, motionally averaged chemical shifts, and identical motionally averaged dipolar couplings to the <sup>31</sup>P nucleus. In principle, REDOR data will be dependent on the angle between the axis of threefold symmetry of the CF<sub>3</sub> group and the vector pointing from the <sup>31</sup>P nuclear coordinate to the “pseudo-atom” center of the CF<sub>3</sub> group. The Schaefer group provided simulations of <sup>31</sup>P{<sup>19</sup>F<sub>3</sub>} REDOR data in this present work include angles of 0° and 90°, the extreme cases.

### 2.4. Determination of error bars in experimental data and uncertainty in distance measurements

The experiments were repeated a minimum of 2–3 times, averaged, and the standard deviation calculated. The error bars in the S/S<sub>0</sub> REDOR dephasing plots were determined by reproducibility of the experiment.

The uncertainty of the distances measured by <sup>31</sup>P{<sup>19</sup>F or <sup>19</sup>F<sub>3</sub>} REDOR for samples **1–6** were calculated by determining the χ<sup>2</sup> and calculating the variation of χ<sup>2</sup> near a minimum as defined in Bevington [20]. Briefly, the minimum of χ<sup>2</sup> was determined by fitting three points that straddle the minimum of χ<sup>2</sup> vs. distance to

#### A S<sub>0</sub> experiment



#### B S experiment

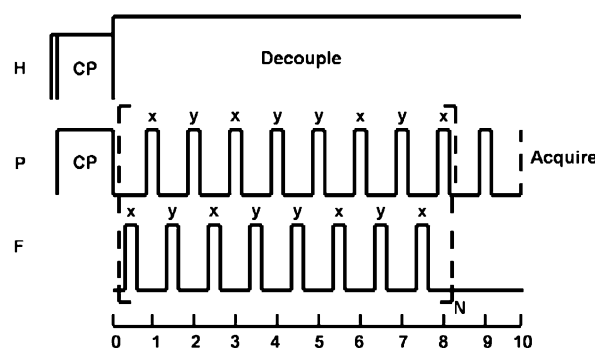


Fig. 3. The XY8-REDOR pulse sequence for measuring <sup>31</sup>P–<sup>19</sup>F dipolar couplings. (A) The S<sub>0</sub> (full echo) experiment shows that following CP from <sup>1</sup>H to <sup>31</sup>P, the phosphorus signal is refocused by a series of π pulses following the XY8 phase cycling. (B) On alternate scans, the S (reduced echo) experiment is collected. The <sup>19</sup>F π pulses are used to recouple the fluorine to the phosphorous nuclei. N is the number of XY8 cycles.

a quadratic equation, and the uncertainty of the distance was measured by taking the second derivative of  $\chi^2$  with respect to the distance [20].

### 3. Results and discussion

#### 3.1. Orientation and theoretical dephasing curves of $-\text{CF}_3$ group

The orientation of the fluorines from a  $-\text{CF}_3$  group with respect to the phosphorous atom can range from  $0^\circ$  to  $90^\circ$ . Fig. 4A depicts the  $0^\circ$  orientation where the  $^{31}\text{P}$  atom lies along the  $\text{C}_3$  axis of the  $-\text{CF}_3$  group while the  $90^\circ$  orientation shown in Fig. 4B is where the  $^{31}\text{P}$  atom is in the plane of the three fluorines. In both orientations, the distance simulated is from the center of mass of the three fluorines to the  $^{31}\text{P}$  atom.

The simulated  $^{31}\text{P}$ – $^{19}\text{F}$  REDOR dephasing curves for P–F and P– $\text{CF}_3$  are compared at several distances 6, 9, and 12 Å in Fig. 5. For each distance, there are three simulated curves, where the solid line represents the dephasing for a given distance between a  $^{31}\text{P}$  atom and a single  $^{19}\text{F}$  atom. The short dashed and dashed lines describe the P– $\text{CF}_3$  simulations where the  $\text{C}_3$  axis of the  $-\text{CF}_3$  group is oriented at its extreme of either  $0^\circ$  or  $90^\circ$  with respect to the  $^{31}\text{P}$  atom, respectively. At 6 Å, the P–F and P– $\text{CF}_3$  dephasing curves are similar to one another. For the 9 and 12 Å dephasing curves, the P– $\text{CF}_3$  curves show greater dephasing than the P–F curves.

At distances greater than 12 Å, the REDOR dephasing curve shows a decreasing dependence upon the orientation of the  $-\text{CF}_3$  group to the point that the apparent dephasing is nearly the same. However, at short distances ( $\sim 6$  Å), the dephasing is more sensitive to the orientation of the  $\text{CF}_3$  group. Fig. 5 shows that

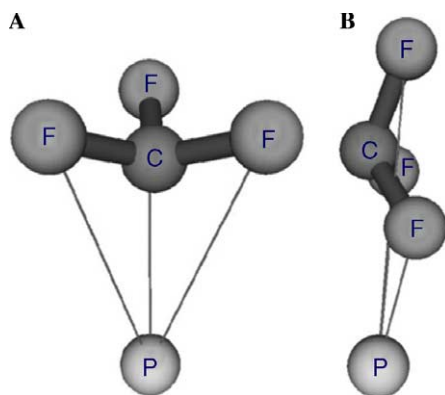


Fig. 4. The orientation of the  $-\text{CF}_3$  group with respect to the phosphorous atom. (A) The P– $\text{CF}_3$   $0^\circ$  orientation is defined as the phosphorous atom being along the  $\text{C}_3$  axis of the  $-\text{CF}_3$  group. (B) The P– $\text{CF}_3$   $90^\circ$  orientation is defined as the phosphorous atom being in the plane of the three fluorines.

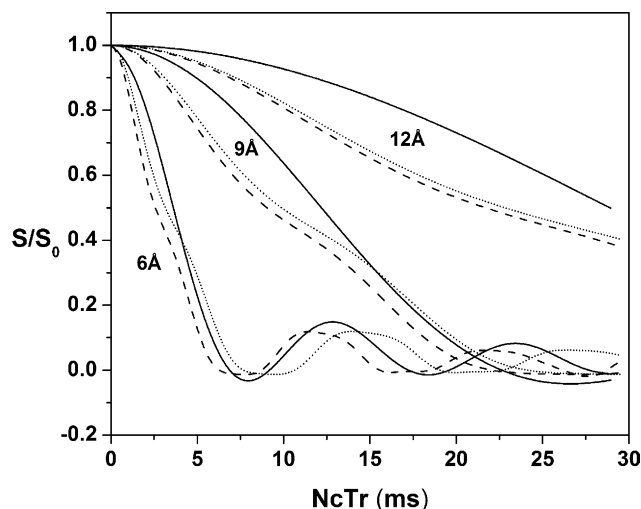


Fig. 5.  $^{31}\text{P}\{^{19}\text{F}\}$  REDOR dephasing curves for P–F and P– $\text{CF}_3$  simulations at 6, 9, and 12 Å. Dashed lines P– $\text{CF}_3$   $90^\circ$ ; dotted line P– $\text{CF}_3$   $0^\circ$ ; and solid line P–F. The dephasing curve is the ratio of the  $S$  and  $S_0$  experiments as a function of  $\text{NcTr}$  which is the number of rotor cycles ( $\text{Nc}$ ) multiplied by the rotor period ( $\text{Tr}$ ).

at 6 Å, the  $90^\circ$  orientation dephases faster than the  $0^\circ$  orientation. At short distances, the difference in distance from the  $^{31}\text{P}$  atom to the center of mass of the three fluorines compared to the distance from the  $^{31}\text{P}$  atom to any one of the fluorines becomes significant, and thus the orientation of the  $-\text{CF}_3$  group is relevant as compared to the distances, where the orientation is irrelevant. At longer distances ( $>12$  Å), the three fluorines of the  $-\text{CF}_3$  group collectively can thus be considered as a “pseudo-atom.”

#### 3.2. Model compounds

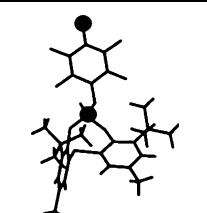
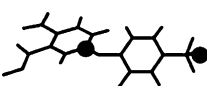
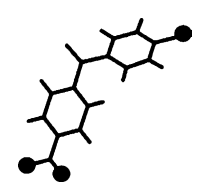
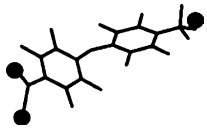
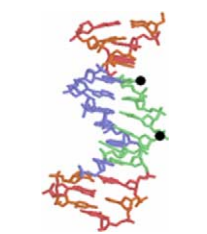
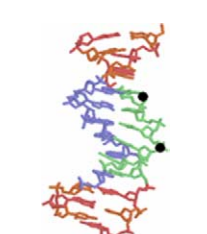
Model compounds were needed to check experimental parameters and to ensure the accuracy of the distances measured by  $^{31}\text{P}\{^{19}\text{F}\}$  REDOR. Several model compounds were synthesized and investigated in this study. Fig. 1 shows the model compounds (1–4) that were synthesized, each contained either a unique fluorine atom or  $-\text{CF}_3$  group and phosphorous atom. The synthetic pathway of compounds 1–4 is shown in Fig. 2. Compounds 1 and 2 were specifically designed such that the internuclear distance between  $^{31}\text{P}$  and  $^{19}\text{F}$  does not vary due to bond rotations. Compounds 3 and 4 were synthesized to measure a longer distance than 1 and 2, however, the distance for both 3 and 4 have an approximate 1.5 Å range due to possible rotation of the C–O bond attached to the phosphate group. The choice of model compounds was based on structural similarity such that the dephasing profile of a compound with one fluorine could be compared to a similar compound where a  $-\text{CF}_3$  group replaces a single  $-\text{F}$  spin.

Two separate sources were used to determine the theoretical  $^{31}\text{P}$  to  $^{19}\text{F}$  distances of the model compounds in

the study. The first method involves searching the Cambridge Structure Database (CSD) for compounds or fragments of the compounds similar to **1–4**. The distances

based on CSD data for structurally similar fragments were compared with the measured distances of the model compounds (**1–4**). Table 1 shows the structures of the

Table 1  
Comparison of distances measured of **1–6** by X-ray crystal structures and  $^{31}\text{P}\{^{19}\text{F}\}$  REDOR

Sample from Fig. 1	Measured distance $r_{\text{P-F}}$ (Å) <sup>a</sup>	X-ray crystal structure, code, and distance $r_{\text{P-F}}$ (Å)
<b>1</b>	6.0 ± 0.9 (1:100 mol/mol KBr) 6.2 ± 1.0 (1:5 mol/mol benzoic acid) 6.0 ± 1.0 (1:20 mol/mol benzoic acid)	HOGDOW <sup>c</sup> 6.66 
<b>2</b>	6.0 ± 0.8 (1:100 mol/mol KBr)	FIPXIL <sup>d</sup> 7.08 
<b>3</b>	9.0 ± 0.9 (undiluted) 9.5 ± 1.1 (10 mg/30 μL) 9.3 ± 1.8 (10 mg/60 μL)	WADBEI <sup>e</sup> 10.31 <sup>b</sup> 
<b>4</b>	8.3 ± 3.7 (undiluted) 9.3 ± 2.7 (1.40 mol/mol benzoic acid)	IBOMUH <sup>f</sup> 11.14 <sup>b</sup> 
<b>5</b>	12 ± 1 ( $W = 14$ )	1BDN <sup>g</sup> 11.89 
<b>6</b>	13 ± 2 ( $W = 14$ )	1BDN <sup>g</sup> 11.16 

The distance between  $^{31}\text{P}$ – $^{19}\text{F}/^{19}\text{F}_3$  of compounds **1–4** and molecules **5** and **6** were measured using  $^{31}\text{P}$ – $^{19}\text{F}$  REDOR without and with dilution. Fragments of crystal structures found in the Cambridge Structural Database (CSD) to be similar to compounds **1–4** are shown with their corresponding CSD code. The crystal structure for molecules **5** and **6** was found in the Protein Data Bank (PDB). The dots in the structures represent the placement of the  $^{31}\text{P}$  and  $^{19}\text{F}$  or center of mass of the  $\text{CF}_3$  group. The distance from the crystal structures were tabulated. The DNA samples were hydrated and in B-form.  $W$  represents the hydration amount and is equivalent to the number of water molecules per nucleotide.

<sup>a</sup> Distance measured using  $^{31}\text{P}\{^{19}\text{F}\}$  REDOR.

<sup>b</sup> Distance was averaged due to phosphorous atom could be in either position.

<sup>c</sup> Ref. [29]

<sup>d</sup> Ref. [30].

<sup>e</sup> Ref. [31].

<sup>f</sup> Ref. [32].

<sup>g</sup> Ref. [25].

crystal fragment with the CSD codes, as well as the distance measured between the phosphorous and fluorine or  $-\text{CF}_3$  group labels, which are identified as dots on the structure. The REDOR results are discussed below whereby the change in dephasing between the single  $-\text{F}$  and  $-\text{CF}_3$  analogues are compared. The second method was a structural minimization using a semi-empirical AM1 closed shell calculation with software provided by Cambridge Soft Corporation. The calculated measurements were used to approximate intermolecular couplings in the model compounds because the fragments of the crystal structures found were not adequate in determination of the next nearest neighbor.

### 3.3. Dephasing differences between $-\text{F}$ and $-\text{CF}_3$

In a  $^{31}\text{P}$ – $^{19}\text{F}$  spin system, REDOR recouples the direct dipolar coupling between the two nuclei. This coupling is quantified as a dephasing of spin coherences of the observed nucleus (e.g.,  $^{31}\text{P}$ ) caused by the coupled spin (e.g.,  $^{19}\text{F}$ ). The amount of dephasing observed is directly related to the internuclear distance of the two spins by the heteronuclear dipolar coupling. Fig. 6, for example, shows a plot of P–F and P– $\text{CF}_3$  distances for a range of coupling constants. At a dipolar coupling of 3 Hz, the difference in distance measurable by P–F and P– $\text{CF}_3$  methods can be as great as 5 Å. Due to limitations of sample size or rotor size as in solid-state NMR experiments, evolution times of about 20 ms are needed for complete dephasing of a P–F sample at a modest distance of 9 Å. By replacing a single fluorine spin with three fluorine spins of a trifluoromethyl group, the dephasing is increased, and thus a longer internuclear distance can be measured at a shorter evolution time.

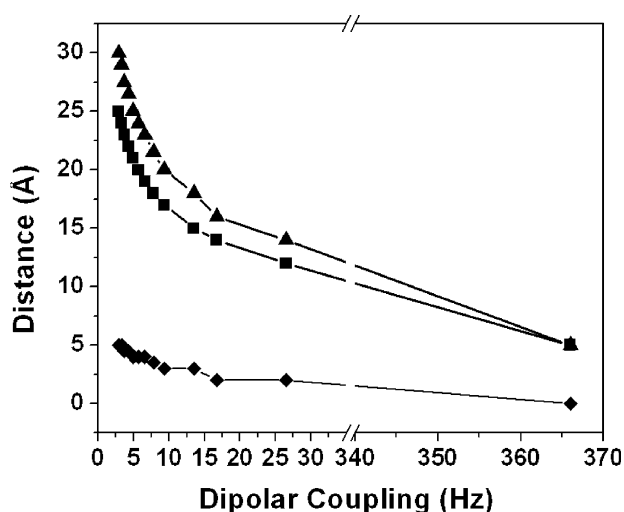


Fig. 6. Comparison of P–F and P– $\text{CF}_3$  distances for a range of coupling constants. As the coupling constant decreases, the difference in distance measurable between the P–F (solid triangles) and P– $\text{CF}_3$  (solid squares) increases to a maximum of 5 Å. Solid diamond shows difference in distance between P–F and P– $\text{CF}_3$ .

REDOR  $S_0$  (full echo) spectra with eight rotor cycles of evolution are shown in Figs. 7A and B for compound **1** undiluted and diluted in benzoic acid (1:40 mol/mol), respectively. The REDOR dephasing curves for the model compounds (1–4) are shown in Figs. 8A and B. In Fig. 8A, the experimental data are shown for compounds **1** and **2** (both diluted in KBr 1:100), along with the 6 Å calculated dephasing curves for P–F and P– $\text{CF}_3$  simulations at  $0^\circ$  and  $90^\circ$ . The X-ray crystal structure distances for compounds **1** and **2** are 6.66 and 7.08 Å, respectively. For compound **1**, the data points follow the 6 Å P–F dephasing curve. The experimental data for **2** fits the calculated dephasing curve of P– $\text{CF}_3$  at  $90^\circ$  up to about 4 ms, and then at longer dephasing times, the data points no longer follow the 6 Å  $\text{CF}_3$   $90^\circ$  dephasing curve and begin to dephase more slowly.

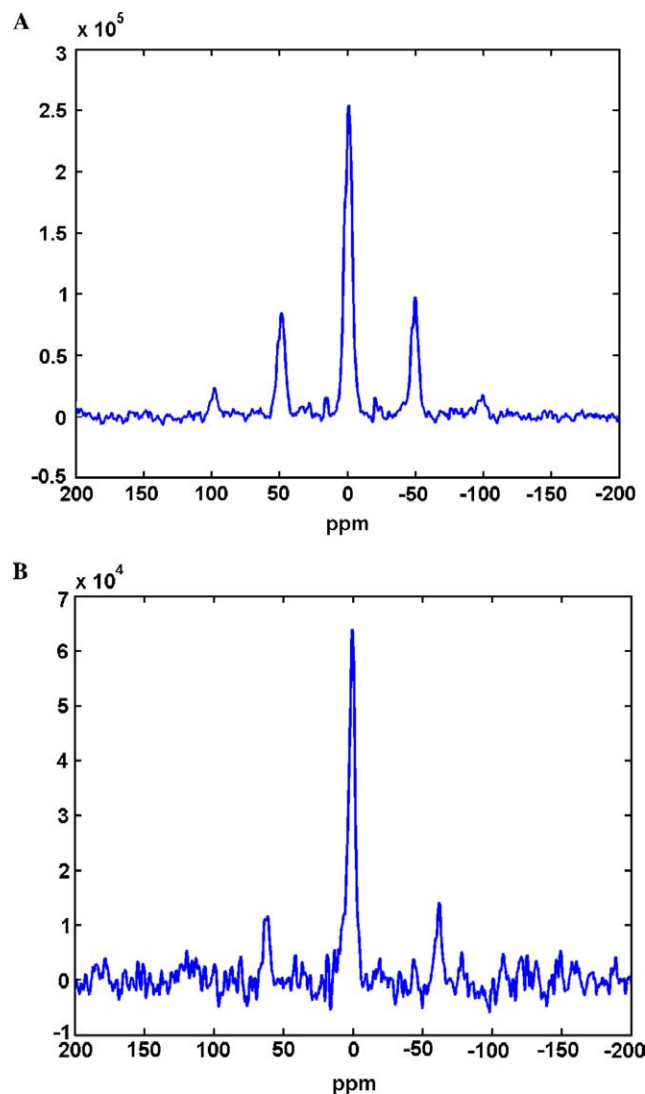


Fig. 7. (A) REDOR  $S_0$  (full echo) spectrum with 8 rotor cycles of evolution for compound **4** undiluted spinning at 4 kHz, 2048 scans. (B) REDOR  $S_0$  (full echo) spectrum with 8 rotor cycles of evolution for compound **4** spinning at 5 kHz diluted 1:40 mol/mol benzoic acid.

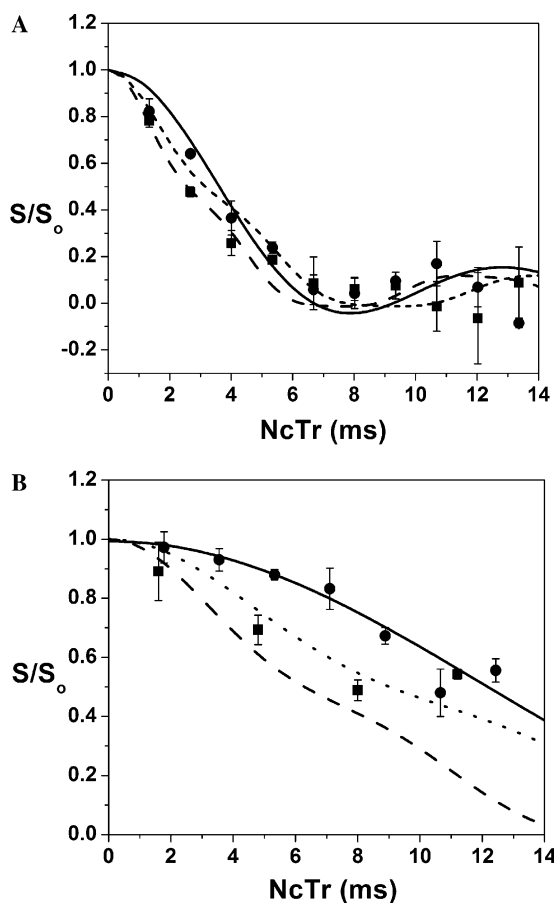


Fig. 8. Overlay of  $^{31}\text{P}\{^{19}\text{F}\}$  REDOR dephasing curves of samples with  $-\text{F}$  and  $-\text{CF}_3$  and simulations. (A) Experimental data for molecules **1** (filled circles) and **2** (filled squares). Both samples were diluted with KBr (1:100). The lines are simulated REDOR curves where the solid line is P–F at 6 Å, short dashed lines are P– $\text{CF}_3$  at 6 Å  $0^\circ$ , long dashed lines are P– $\text{CF}_3$  at 6 Å  $90^\circ$ . (B) Experimental data for molecules **3** (filled circles) diluted 1:40 in benzoic acid and **4** (filled squares) diluted 10 mg/60  $\mu\text{L}$  in  $\text{H}_2\text{O}$ . The lines are simulated REDOR curves, solid line is P–F at 9 Å, short dashed lines are P– $\text{CF}_3$  at 9 Å  $90^\circ$ , and long dashed lines are P– $\text{CF}_3$  at 8 Å  $90^\circ$ .

In addition, **1** was also diluted in benzoic acid at ratios of 1:5 and 1:20 mol/mol. Regardless of the dilution method, the average distances measured for **1** and **2** were shorter than the X-ray crystal distance as shown in Table 1. The crystal structure distance was within the experimental uncertainty of compound **1** but not within the uncertainty for compound **2**.

Compounds **3** and **4** were diluted in deionized water (10 mg/30  $\mu\text{L}$  and 10 mg/60  $\mu\text{L}$ ) and 1:40 mol/mol benzoic acid, respectively. Fig. 8B shows the dephasing curve for **3** diluted in deionized water at a concentration of 10 mg/60  $\mu\text{L}$  and **4** diluted with 1:40 mol/mol benzoic acid. The experimental data for **3** best fits the 9 Å P–F dephasing curve and **4** fits between the 8 and 9 Å  $90^\circ$  P– $\text{CF}_3$  dephasing curves. Similar to compounds **1** and **2**, **3** and **4** also show a shorter measured distance of about 9.3 Å compared to the crystal structure fragment distance of 10.31 and 11.14 Å, respectively. As longer in-

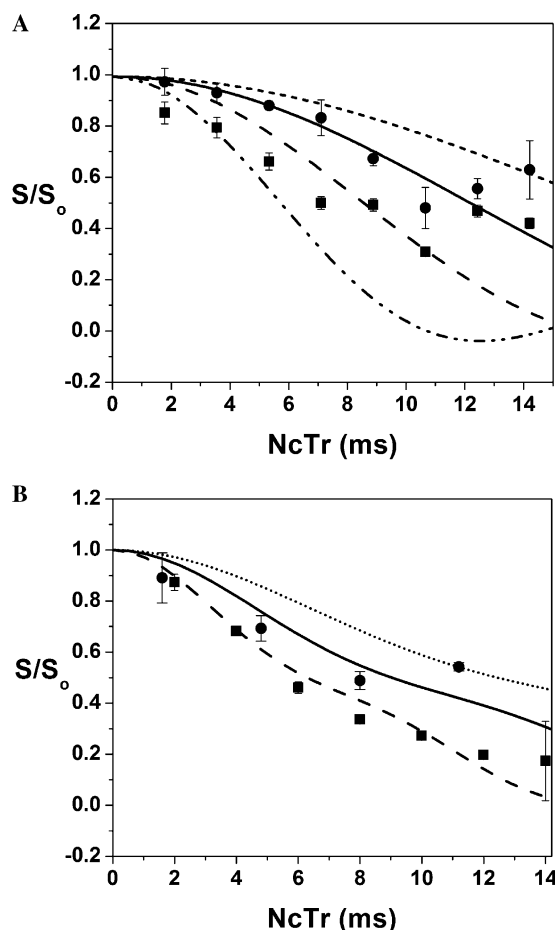


Fig. 9. (A) Experimental data for compound **3** undiluted (solid squares) and diluted (solid circles) in distilled water at 10 mg/60  $\mu\text{L}$ . The lines are simulated REDOR curves for P–F at 7, 8, and 9 Å. (B) Experimental data for compound **4** undiluted (solid triangles) and diluted (solid diamonds) in 1:40 mol/mol benzoic acid. The lines are simulated REDOR curves for P– $\text{CF}_3$   $90^\circ$  at 8, 9, and 10 Å.

ter-label distances were measured, there was a larger disparity between the crystal structure fragment measurement and to the  $^{31}\text{P}\{^{19}\text{F}\}$  REDOR distances. In addition, the experimental uncertainty for molecules **3** and **4** in some cases was greater than 1 Å, and probably due to heterogeneity in conformation of the sample from rotation of the phosphate group and perhaps the multiple spin couplings from intermolecular effects. The rotation of the C–O bond of the phosphate group for **3** and **4** can possibly contribute a 1.2–1.5 Å range in the observed distance.

McDermott and co-workers [7] have used model fluorinated compounds to measure  $^{19}\text{F}$ – $^{19}\text{F}$  internuclear distances via RFDR. Their solution for avoiding intermolecular dipolar couplings from neighboring fluorinated compounds was the dilution of fluorinated compounds by co-crystallization with nonfluorinated analogues that were structurally similar. In our study, various dilution methods were attempted. For model compound **1**, the dilution methods used were diluting



1:100 mol/mol in KBr, 1:5 and 1:20 mol/mol in benzoic acid. None of the dilution methods showed a significant change in distance measured as reported in Table 1. Thus, for compound **2**, the only dilution method used was 1:100 mol/mol KBr. Another dilution method was tried for compound **3**. In Fig. 9A, the REDOR dephasing curves are shown for compound **3** undiluted and diluted in a solution of deionized water at a concentration of 10 mg/60  $\mu$ L. Comparison of the undiluted case and the diluted cases of compound **3** demonstrates a distance change from 9.0 to 9.3 Å, respectively. The dephasing curves in Fig. 9A show that there is a visible dephasing difference and that dilution of the compound in deionized water has some effect in isolating the phosphorous and fluorine spins. Likewise, Fig. 9B shows the dephasing curves of compound **4** undiluted and diluted in 1:40 mol/mol benzoic acids, and also illustrates that dilution of **4** in 1:40 benzoic acid isolates the phosphorous and fluorine spins to some extent.

Attempts were made to dilute the samples further such that intermolecular couplings might be reduced. However, as dilution of sample increased, the signal-to-noise diminished and experimental points were more scattered at long dephasing times. It has been noted that small fluorinated compounds tend to aggregate and do not make good model compounds (M.E. Merritt personal communication) [14]. McDermott et al. [7] also encountered inhomogeneous or inadequate dilution of samples with their fluorinated model samples. In addition, halogenated organic crystals are also known to aggregate [21,22]. Thus, it is suspected that these apparent intermolecular couplings may be due to aggregation of the fluorines and use of an insufficient molecular mixing method.

### 3.4. Multiple spin simulations and fits

To address the issue of the experimental distances being shorter than the calculated distances for the compounds **1–4**, simulations using SIMPSON [23] were performed to describe possible packing models of the compounds where the intermolecular effects give rise to a distribution of distances and thus, multi-spin effects.

For compound **1**, the energy minimized structure obtained from the AM1 calculation was put in a fictitious cubic crystal cell (Cell constant 10 Å) in the Weblab Viewerlite Visualization program by Accelrys. This calculation showed the possibility of an intermolecular  $^{31}\text{P}\text{--}^{19}\text{F}$  distance of 3.5 Å that can be seen in Fig. 10A. Assuming partial aggregation causing intermolecular effects, the experimental data were fit to a linear combination of two spin and three spin simulations. The best fit occurred at a 90% of a  $^{31}\text{P}\text{--}^{19}\text{F}$  distance of 6 Å and 10% of  $^{31}\text{P}\text{--}^{19}\text{F}$  distances of 6 and 3.5 Å as shown in Fig. 10B.

For compound **2**, the distances obtained from a semi-empirical AM1 closed shell calculation are 7.26, 7.36, and 7.64 Å for the three fluorine atoms, respectively, from the phosphorus atom. The simulated result is co-plotted with compound **1** in Fig. 10B. The best fit simulation considered the center of the  $\text{CF}_3$  to be 5.34 Å as opposed to the expected 7.42 Å distance from the AM1 calculation. This discrepancy is mostly due to aggregation leading to spin diffusion. Most recent work shows that in cases where multiple dephasers are involved simulation of data requires the exact molecular geometry [28]. Despite the experimental distances being shorter than the calculated distances, the dephasing of compound **2** was greater than compound **1**, as expected due to the  $\text{--CF}_3$  group in compound **2**.

The AM1 minimized structure for compound **3** suggested that the P–F distance could range between 9.8 and 11.5 Å depending upon the torsion angle of the phosphate group. The  $^{31}\text{P}\{^{19}\text{F}\}$  REDOR data of the undiluted sample of **3** could not be fit to a single distance. For compound **3**, when diluted to 10 mg/30  $\mu$ l, the REDOR dephasing could be fit to a single distance of 9.2 Å. This shorter distance obtained from the REDOR experiment is probably due to the presence of intermolecular  $^{31}\text{P}\text{--}^{19}\text{F}$  couplings. For example, the curve could be fit to a linear combination of two REDOR curves, one due to a single spin at 9.8 Å distance contributing 67% and another due to two spins at distances 9.8 and 9.0 Å, respectively, with the 9.0 Å being the distance between the phosphorus and a fluorine from another molecule. These results are shown in Fig. 10C.

For **4**, the expected distance of 10.9 Å from the AM1 structure minimization correlated with three P–F couplings of 34, 39, and 49 Hz. The experimental data for **4** diluted with benzoic acid (1:40) was best fit to three P–F couplings of 89, 93, and 122 Hz. Again, in this case the fitted distances were much shorter than the expected distance as determined from the AM1 calculation.

### 3.5. Fluorinated and trifluoromethylated DNA samples

The sequences and labeling scheme of the fluorinated DNA (**5** and **6**) used in this study are shown in Fig. 1. The structure of the DNA sequence was selected because it was not self-complementary and the X-ray crystal structure was published in the Protein Data Bank (PDB) [24] as code 1BDN [25]. A self-complementary sequence would complicate the analysis due to inter- and intrastrand interactions. The DNA were synthetically modified to accommodate a fluorine or  $\text{--CF}_3$  group and phosphorothioate for the  $^{31}\text{P}\{^{19}\text{F}\}$  REDOR dephasing comparison studies. Thermodynamic data for DNA duplexes with and without a trifluoromethylated label were compared and previously reported by Markley et al. [12]. Optical melting experiments were performed and it was found that DNA duplex stability

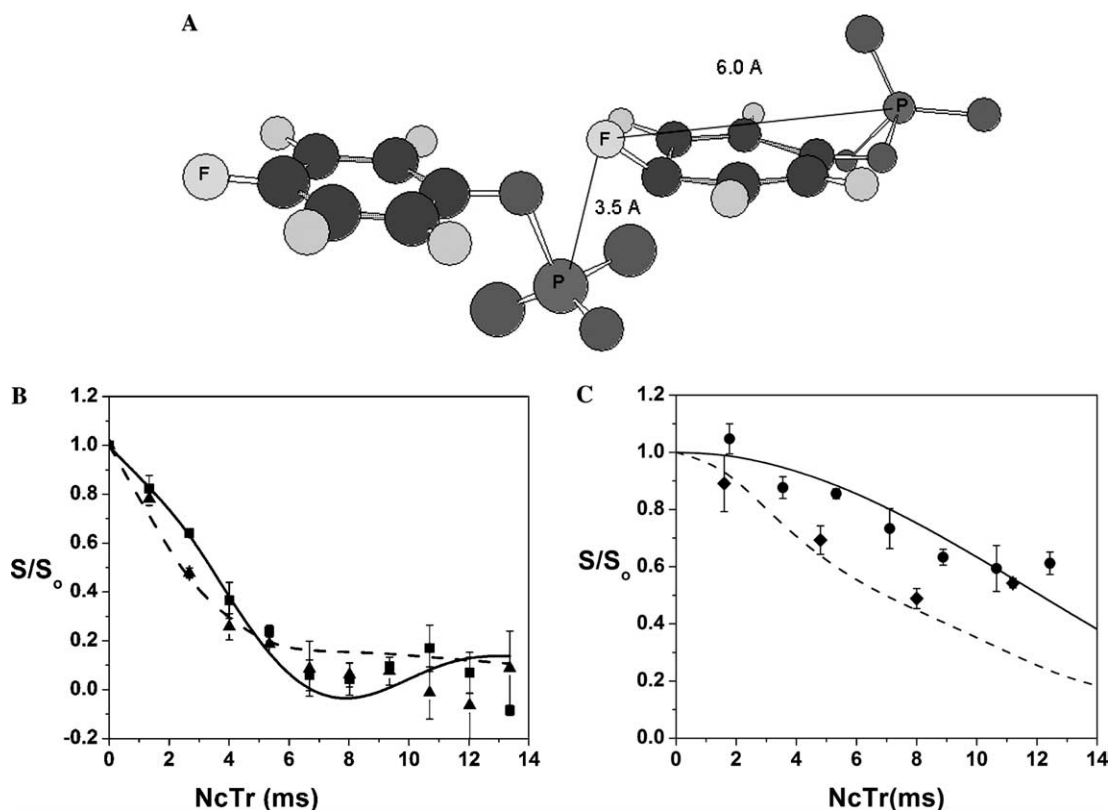


Fig. 10. Multi-spin model, simulations, and dephasing curves. (A) Model for multi-spin simulation of **1** where the  $^{19}\text{F}$  atom is coupled to  $^{31}\text{P}$  at 6.0 and 3.5 Å. (B) Experimental data for **1** (solid square) diluted with KBr (1:100). The dashed line represents the best fit to a linear combination of two spin (90% 6 Å) and three spin simulations (10% of 6 and 3.5 Å). Experimental data for **2** (solid triangle) diluted with KBr (1:100). The best fit simulation considered a  $-\text{CF}_3$  at a distance of 5.34 Å. (C) Experimental data for **3** (solid circle) diluted 10 mg/30  $\mu\text{L}$  in  $\text{H}_2\text{O}$ . The curve was fit to a linear combination of two REDOR effects, one due to a single spin at 9.8 Å distance contributing 67% and another due to two spins at distances 9.8 and 9.0 Å, respectively, with the 9.0 Å being the distance from the phosphorus and a fluorine from another molecule. Experimental data for **4** (solid diamond) diluted with benzoic acid (1:40). The dashed line represents the best fit to a four spin simulation (89, 93, and 122 Hz).

at pH 6.9 was lowered slightly (a  $T_m$  difference of 3 °C) due to the incorporation of the trifluoromethyl group [12].

Based on the crystal structure data, the phosphorothioate and  $-\text{F}$  or  $-\text{CF}_3$  labels in the duplex DNA were designed to be 12 Å apart. Fig. 11 is the  $^{31}\text{P}\{^{19}\text{F}\}$  REDOR  $S_0$  spectrum of dsDNA **5** showing the phosphorothioate peak chemically shifted upfield 55 ppm from the phosphate backbone. The sample was spun at 5988 Hz in order to allow for adequate resolution between the spinning sideband peak of the backbone phosphates and the phosphorothioate peak. For the dsDNA samples, **5** and **6**, the dephasing curves are shown in Figs. 12A and B, respectively. The data points for the dsDNA sample, **5**, fall between the 11 and 13 Å P-F dephasing simulations. A  $\chi^2$  plot vs. distance is shown in the inset of Fig. 12A where the equation of a parabola was fit to pass through three points that straddle the minimum. From the parabolic fit, the  $\chi^2$  minimum and standard deviation can be determined [20]. The best fit for **5** was  $12 \pm 1$  Å, which is in good agreement with the crystal structure distance of 11.89 Å. In the case of the dsDNA with the  $-\text{CF}_3$  group, **6**, the  $^{31}\text{P}\{^{19}\text{F}\}$  REDOR

experimental points were between the 10 and 14 Å P- $\text{CF}_3$  90° simulations as shown in Fig. 12B. The  $\chi^2$  is shown in the inset of Fig. 12B, and the minimum  $\chi^2$  and standard deviation was determined to be  $13 \pm 2$  Å, which is also in agreement with the X-ray crystal structure. In addition, by co-plotting the experimental data points of **5** and **6**, as in Fig. 12C, the difference in dephasing behavior between the single  $-\text{F}$  and  $-\text{CF}_3$  dsDNA is demonstrated, especially at 20 ms.

The intermolecular coupling effects were not observed in the dsDNA samples, likely due to the oligomers self-diluting. The ratio of distance measured to length of the molecule is smaller than the model compounds **1–4**. The P-F and P- $\text{CF}_3$  labels were strategically placed so that the distance of the labels would be shorter than the length of the duplex 12 mer DNA. This may have contributed to a more accurate distance measurement by preventing intermolecular couplings and better isolating the P-F and P- $\text{CF}_3$  spin pairs. The distance of the P-F or P- $\text{CF}_3$  labels in **1–4** were essentially the length of the molecule, and therefore contributed to intermolecular effects creating an apparent faster dephasing.

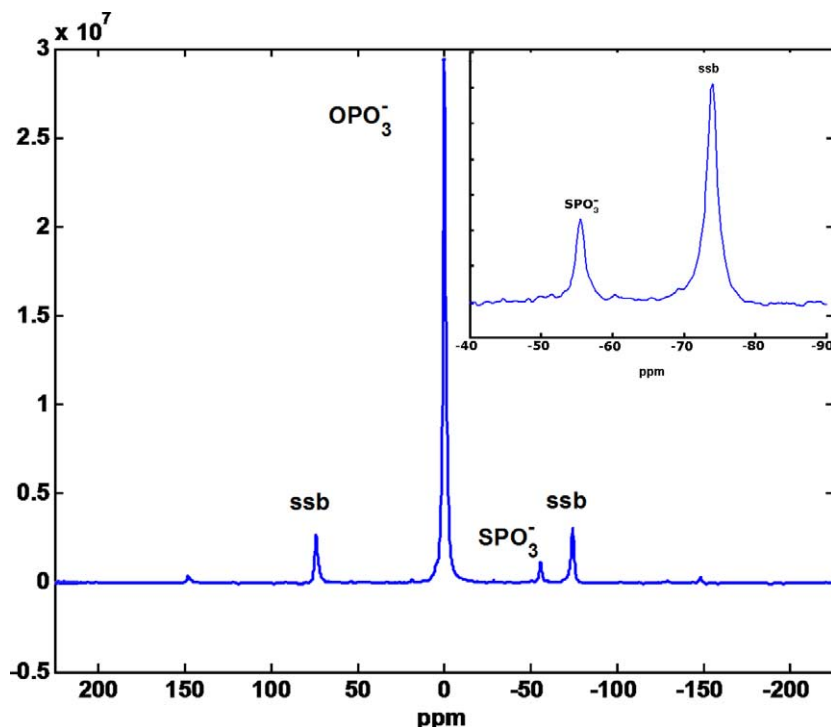


Fig. 11. REDOR  $S_0$  (full echo) spectrum with 8 rotor cycles of evolution for  $5'/\text{d}(\text{CGCATT}-(\text{pS})\text{-TT}^{5\text{-F}}\text{UGCG})\text{-d}(\text{CGCAAAAATGCG})$  where  $5\text{-F}^{\text{U}}$  denotes 2'-deoxy-5-fluorouridine and (pS) denotes a phosphorothioate ( $\text{SPO}_3^-$ ) in place of a phosphate ( $\text{OPO}_3^-$ ) group. Magic-angle spinning was performed at  $5988 \pm 2$  Hz. Three sets of 6144 scans were acquired. The spinning sidebands are labeled  $\text{ssb}$ . Inset shows phosphorothioate peak and spinning sideband.

### 3.6. Advantages and disadvantages of $-\text{CF}_3$

In deciding when to include a  $-\text{CF}_3$  group or  $-\text{F}$  in a sample, the choice depends on the information desired, the system of interest, and placement of the label. Besides the ability to measure a long-range distance with a  $-\text{CF}_3$  group, there is an advantage of a  $-\text{CF}_3$  group at short distances, as well. For distances not more than  $\sim 6$  Å, dephasing is sensitive to the orientation of the  $-\text{CF}_3$  group relative to the phosphorous nucleus, if the error in the dephasing data points is low. Fig. 8A illustrates that the  $6$  Å  $0^\circ$  and  $90^\circ$  dephasing curves are sufficiently distinguishable to allow determination of the orientation of the  $-\text{CF}_3$  group relative to the phosphorous nucleus. The first three experimental points of the dephasing curve of **2**, indicated by solid squares, are in good agreement with the theoretical  $\text{P}-\text{F}_3$   $6$  Å  $90^\circ$  dephasing curve (long dashes). Due to the  $\text{C}-\text{O}-\text{P}$  arrangement as in molecule **2**, the  $-\text{CF}_3$  group is situated  $90^\circ$  relative to the phosphate atom, which is in agreement with the experimental result. As a result of intermolecular couplings, at longer dephasing times (greater than 5 ms), the experimental results no longer follow the  $6$  Å  $90^\circ$  dephasing curve. At distances greater than  $6$  Å, the theoretical  $\text{P}-\text{F}_3$   $0^\circ$  and  $90^\circ$  dephasing curves begin to converge and the orientation of the  $-\text{CF}_3$  group can no longer be distinguished. Thus, as seen in the results, there can be a disadvantage to incor-

porating a  $-\text{CF}_3$  group when the molecule of interest is inadequately diluted and/or the distance measured is large compared to the size of the molecule due to intermolecular effect. Thus, the  $-\text{F}$  label is best used when measuring short distances in order to avoid intermolecular effects. Despite the inadequate molecular mixing causing aggregation or poor dilution of the spins, for compounds **1-4**, it was shown that replacing a  $-\text{F}$  with a  $-\text{CF}_3$  group allowed the dephasing behavior to increase. This trend of increased dephasing was also seen with the dsDNA samples of **5** and **6**. A greater apparent dephasing due to the  $\text{CF}_3$  substitution will allow for longer distance measurement especially when working with biological samples in  $\mu\text{mol}$  scale quantities.

### 3.7. Limit of $\text{P}-\text{CF}_3$ coupling

Table 2 is a theoretical comparison of the amount of dephasing between  $\text{P}-\text{F}$  and  $\text{P}-\text{F}_3$  and shows that a distance of  $20$  Å has 8% dephasing after 30 ms [26,27] evolution for a  $\text{P}-\text{F}_3$  system, which is an estimate of the upper limit of the distance measurable using a  $-\text{CF}_3$  group in place of a  $-\text{F}$ . The Schaefer group [3] has measured a maximum distance of  $16$  Å (12 Hz) using  $\text{P}-\text{F}$  REDOR. According to Table 2,  $\text{P}-\text{CF}_3$  coupling of 12 Hz correlates to a  $19$  Å. This implies that it is possible to measure a  $19$  Å distance with  $\text{P}-\text{CF}_3$  REDOR.

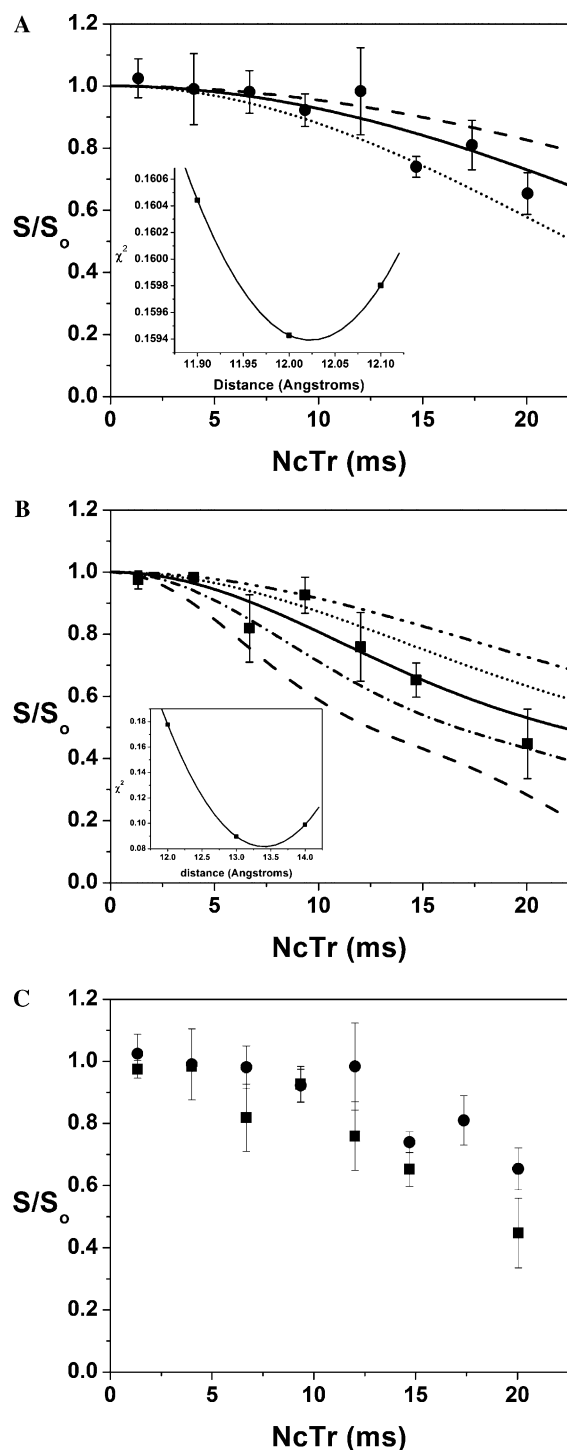


Fig. 12.  $^{31}\text{P}\{^{19}\text{F}\}$  REDOR dephasing curves for dsDNA. (A) Dots are experimental data for dsDNA with single fluorine (**5**). The lines are simulated  $^{31}\text{P}\text{-}^{19}\text{F}$  dephasing curves: dots 11 Å (34 Hz), solid line 12 Å (26 Hz), and dashed lines 13 Å (21 Hz). Inset is of  $\chi^2$  vs. distance. (B) short dashed lines are P- $\text{CF}_3$  at 12 Å  $0^\circ$ , long dashed lines are P- $\text{CF}_3$  at 12 Å  $90^\circ$ . Inset is of  $\chi^2$  vs. distance. (C) Co-plot of  $^{31}\text{P}\{^{19}\text{F}\}$  REDOR dephasing curves for dsDNA **5** (solid circles) and **6** (solid squares) where the DNA with the  $-\text{CF}_3$  (**6**) incorporated shows more dephasing than the DNA with a single fluorine (**5**) especially the data points at 20 ms shows the increase in dephasing due to the  $\text{CF}_3$  group.  $\text{CF}_3$  dephased 60%, CF dephased 35% at 20 ms.

Table 2

A comparison of the percent dephasing of P-F and P- $\text{CF}_3$  at 30 ms evolution

Distance (Å)	Percent dephasing	
	P-F	P- $\text{CF}_3$
6	100	100
9	100	100
11	73	80
13	50	60
15	15	35
16		26
18	5.5	15
20	3	8
23	1.2	4
27	0.5	1.5
30	0.3	0.8

### 3.8. Effective gamma for "Super" fluorine in $-\text{CF}_3$ group

The same dipolar coupling for P- $\text{CF}_3$  and P-F yield different distances due to their difference in dephasing behaviors. Due to the proportional relationship of the gyromagnetic ratios and the dipolar coupling, an average effective gyromagnetic ratio for the fluorines in the  $-\text{CF}_3$  group was estimated using  $\gamma_{\text{P-}\text{CF}_3} = \gamma_{\text{P-F}}[(r_{\text{P-}\text{CF}_3})_3 / (r_{\text{P-F}})_3]$ . The  $^{19}\text{F}$  gyromagnetic ratio is 25,182 1/(G s) and for the same dipolar coupling, a ratio of the distances  $(r_{\text{P-}\text{CF}_3})^3 / (r_{\text{P-F}})^3$  can be determined. The effective gyromagnetic ratio for the fluorines in a  $-\text{CF}_3$  group for several dipolar couplings was averaged to be  $42,556 \pm 2000$  1/(G s). Thus, the gyromagnetic ratios of the  $\text{CF}_3$  to F is 1.69:1 which is about a 39% increase.

## 4. Conclusion

$^{31}\text{P}\{^{19}\text{F}\}$  and  $^{31}\text{P}\{^{19}\text{F}_3\}$  REDOR experiments were performed on small model compounds and nucleic acid oligomers. With replacement of a  $-\text{CF}_3$  group for  $-\text{F}$ , the behavior of  $^{31}\text{P}\text{-}^{19}\text{F}$  dephasing was studied. The experimental distances ascertained by  $^{31}\text{P}\{^{19}\text{F}\}$  REDOR for the model compounds, **1-4**, ranged from half to one Angstrom less than the distance calculated from the minimized structure. There was inadequate dilution of the spins and the hindrance was most likely due to the nature of the size of the compound in relation to the distance being measured causing intermolecular effects as well as possible aggregation of the fluorine atoms. The moderate distances measured in the double-stranded 12-mer DNA molecules were self-diluting and thus, the experimental distances were in good agreement with the X-ray crystal structure.

Regardless of the intermolecular effects, in all sets of molecules, samples with a  $-\text{CF}_3$  group consistently exhibited more dephasing than the  $-\text{F}$  sample counterpart. This increase in dephasing indicates that a  $-\text{CF}_3$

group is a more sensitive measure than a single fluorine, and more accurate distance measurements can be assessed at a shorter dephasing time for distances greater than 12 Å, which can be important when studying large biomolecules or biological complexes.

In summary, long-distance constraints of at most 20 Å are theoretically measurable with the  $^{31}\text{P}\{^{19}\text{F}\}$  REDOR technique in nucleic acids by incorporation of a  $-\text{CF}_3$  group and slight modification of the phosphate backbone with one phosphorothioate.

### Acknowledgments

We thank M.E. Merritt for helpful discussions; J. Schaefer and his group members for  $\text{P}-\text{CF}_3$  REDOR simulations, helpful discussions, and comments; T.E. Edwards, J. D. Wellhausen, J. C. Markley, and D. Sologub for synthesizing and purifying the DNA; N.A. Oyler for the use of his Matlab code for the NMR data work-up and the C++ code for the  $\text{P}-\text{F}$  REDOR simulations; and James Gibson for reading repeated revisions of the manuscript. This research was supported by the National Institute of Health. Grants (RO1 EB03152-O5) and (RO1 DE-12554-08) and by NSF Grant (DMR 0110505).

### Appendix A. Supplementary data

Supplementary data associated with this article can be found, in the online version, at [doi:10.1016/j.jmr.2005.06.018](https://doi.org/10.1016/j.jmr.2005.06.018).

### References

- [1] T. Gullion, J. Schaefer, Rotational-echo double-resonance NMR, *J. Magn. Reson.* 81 (1989) 196–200.
- [2] T. Gullion, J. Schaefer, Detection of weak heteronuclear dipolar coupling by rotational-echo double-resonance nuclear magnetic resonance, *Adv. Magn. Reson.* 13 (1989) 57–83.
- [3] D.R. Studelska, C.A. Klug, D.D. Beusen, L.M. McDowell, J. Schaefer, Long-range distance measurements of protein binding sites by rotational-echo double-resonance NMR, *J. Am. Chem. Soc.* 118 (1996) 5476–5477.
- [4] M.E. Merritt, S.T. Sigurdsson, G.P. Drobny, Long-range distance measurements to the phosphodiester backbone of solid nucleic acids using  $\text{P}-31\text{-F}-19$  REDOR NMR, *J. Am. Chem. Soc.* 121 (1999) 6070–6071.
- [5] G.L. Olsen, E.A. Louie, G.P. Drobny, S.T. Sigurdsson, Determination of DNA minor groove width in distamycin–DNA complexes by solid-state NMR, *Nucleic Acids Res.* 31 (2003) 5084–5089.
- [6] J.A. Stringer, G.P. Drobny, Methods for the analysis and design of a solid state nuclear magnetic resonance probe, *Rev. Sci. Instrum.* 69 (1998) 3384–3391.
- [7] M.L. Gilchrist, K. Monde, Y. Tomita, T. Iwashita, K. Nakanishi, A.E. McDermott, Measurement of interfluorine distances in solids, *J. Magn. Reson.* 152 (2001) 1–6.
- [8] L.M. McDowell, D.R. Studelska, B. Poliks, R.D. O'Connor, J. Schaefer, Characterization of the complex of a trifluoromethyl-substituted shikimate-based bisubstrate inhibitor and 5-enolpyruvylshikimate-3-phosphate synthase by REDOR NMR, *Biochemistry* 43 (2004) 6606–6611.
- [9] J.M. Goetz, J. Schaefer, REDOR dephasing by multiple spins in the presence of molecular motion, *J. Magn. Reson.* 127 (1997) 147–154.
- [10] W.H. Gmeiner, R.T. Pon, J.W. Lown, Synthesis, annealing properties,  $\text{F}-19$  NMR characterization, and detection limits of a trifluorothymidine-labeled antisense oligodeoxyribonucleotide 21-Mer, *J. Org. Chem.* 56 (1991) 3602–3608.
- [11] P.D. Cook, Y.S. Sanghvi, US Patent 5,614,617, 1992; *Chem. Abstr.* 1992, 117, 111996., 1992.
- [12] J.C. Markley, P. Chirakul, D. Sologub, S.T. Sigurdsson, Incorporation of 2'-deoxy-5-(trifluoromethyl)uridine and 5-cyano-2'-deoxyuridine into DNA, *Bioorg. Med. Chem. Lett.* 11 (2001) 2453–2455.
- [13] T.M. Alam, G.P. Drobny, Solid-state Nmr-studies of Dna-structure and dynamics, *Chem. Rev.* 91 (1991) 1545–1590.
- [14] J.A. Stringer, *The Design and Analysis of Solid State Nuclear Magnetic Resonance Probes for the Determination of Biomolecular Structure*, University of Washington, 1998.
- [15] J.R. Garbow, T. Gullion, Improvements in Redor NMR-spectroscopy—minimizing resonance-offset effects, *J. Magn. Reson.* 95 (1991) 442–445.
- [16] A.K. Mehta, D.J. Hirsh, N. Oyler, G.P. Drobny, J. Schaefer, Carbon–proton dipolar decoupling in REDOR, *J. Magn. Reson.* 145 (2000) 156–158.
- [17] F.G. Vogt, J.M. Gibson, S.M. Mattingly, K.T. Mueller, Determination of molecular geometry in solid-state NMR: rotational-echo double resonance of three-spin systems, *J. Phys. Chem. B* 107 (2003) 1272–1283.
- [18] T. Gullion, D.B. Baker, M.S. Conradi, New compensated Carr–Purcell sequences, *J. Magn. Reson.* 89 (1990) 479–484.
- [19] Y. Pan,  $\text{P}-31\text{-F}-19$  rotational-echo, double-resonance nuclear-magnetic-resonance experiment on fluoridated hydroxyapatite, *Solid State Nucl. Magn. Reson.* 5 (1995) 263–268.
- [20] P.R. Bevington, D.K. Robinson, *Data Reduction and Error Analysis for the Physical Sciences*, (1992).
- [21] O.V. Grineva, P.M. Zorkii, Aggregation of halogen atoms in haloorganic crystals with low halogen contents, *Russ. J. Phys. Chem.* 74 (2000) 1758–1764.
- [22] O.V. Grineva, P.M. Zorkii, Aggregation of halogen atoms in crystalline isomers, *J. Struct. Chem.* 43 (2002) 995–1005.
- [23] M. Bak, J.T. Rasmussen, N.C. Nielsen, SIMPSON: a general simulation program for solid-state NMR spectroscopy, *J. Magn. Reson.* 147 (2000) 296–330.
- [24] H.M. Berman, J. Westbrook, Z. Feng, G. Gilliland, T.N. Bhat, H. Weissig, I.N. Shindyalov, P.E. Bourne, *The Protein Data Bank*, *Nucleic Acids Res.* 28 (2000) 235–242.
- [25] A.D. Digabriele, M.R. Sanderson, T.A. Steitz, Crystal-lattice packing is important in determining the bend of a Dna dodecamer containing an adenine tract, *Proc. Natl. Acad. Sci. USA* 86 (1989) 1816–1820.
- [26] A.K. Mehta, J. Schaefer, Rotational-echo double resonance of uniformly labeled C-13 clusters, *J. Magn. Reson.* 163 (2003) 188–191.
- [27] L.M. McDowell, A. Schmidt, E.R. Cohen, D.R. Studelska, J. Schaefer, Structural constraints on the ternary complex of 5-enolpyruvylshikimate-3-phosphate synthase from rotational-echo double-resonance NMR, *J. Mol. Biol.* 256 (1996) 160–171.
- [28] G. Goobes, V. Raghunathan, E.A. Louie, J.M. Gibson, G.L. Olsen, G.P. Drobny, REDOR study of diammonium hydrogen phosphate: A model for distance measurements from adsorbed molecules to surfaces. *Solid state Nucl. Magn. Reson.* (2005) in press.

- [29] P. Sood, A. Chandrasekharan, R.O. Day, R.R. Holmes, Structural displacement of phosphites, phosphates, and pentaoxyphosphoranes to higher coordinate geometries by sulfur and oxygen donor action, *Inorg. Chem.* 37 (1998) 6329.
- [30] C.H.L. Kennard, O. Smith, T. Hari, The crystal structure of acifluorfen [5-[2-chloro-4-(trifluoromethyl)phenoxy]-2-nitrobenzoic acid], *Aust. J. Chem.* 40 (1987) 1131.
- [31] S. Guo, G. Su, F. Pan, Y. He, The crystal structure of acifluorfen [5-[2-chloro-4-(trifluoromethyl)phenoxy]-2-nitrobenzoic acid], *Z. Kristallogr.* 202 (1992) 296.
- [32] T.M. Klapotke, B. Krumm, P. Meyer, H. Piotrowski, Synthesis and chemistry of  $\text{CF}_3\text{C}_6\text{F}_4\text{OC}_6\text{F}_4\text{NH}_2$  ( $\text{R}_\text{F}\text{NH}_2$ ) and pseudohalogen derivatives; Crystal structures of  $\text{R}_\text{F}\text{X}$  ( $\text{X} = \text{COOH}, \text{COCl}, \text{CN}, \text{N}_3, \text{NCS}, \text{NHCOCONHR}_\text{F}$ ), *Z. Anorg. Allg. Chem.* 627 (2001) 1983.